

When Does Machine Learning FAIL? Generalized Transferability for Evasion and Poisoning Attacks

Octavian Suciu

Radu Mărginean

Yiğitcan Kaya

Hal Daumé III

Tudor Dumitraş

University of Maryland, College Park

Abstract

Attacks against machine learning systems represent a growing threat as highlighted by the abundance of attacks proposed lately. However, attacks often make unrealistic assumptions about the knowledge and capabilities of adversaries. To evaluate this threat systematically, we propose the **FAIL** attacker model, which describes the adversary’s knowledge and control along four dimensions. The **FAIL** model allows us to consider a wide range of weaker adversaries that have limited control and incomplete knowledge of the features, learning algorithms and training instances utilized. Within this framework, we evaluate the generalized transferability of a known evasion attack and we design *StingRay*, a targeted poisoning attack that is broadly applicable—it is practical against 4 machine learning applications, which use 3 different learning algorithms, and it can bypass 2 existing defenses. Our evaluation provides deeper insights into the transferability of poison and evasion samples across models and suggests promising directions for investigating defenses against this threat.

1 Introduction

Machine learning (ML) systems are widely deployed in safety-critical domains that carry incentives for potential adversaries, such as finance [1], medical field [7], the justice system [37], cybersecurity products [2], or self-driving cars [8]. A ML classifier automatically learns classification models using labeled observations (samples) from a *training set*, without requiring predetermined rules for mapping inputs to labels. It can then apply these models to predict labels for new samples in a *testing set*. A major pursuit of adversarial machine learning is to understand the threat of targeted attacks, where the adversary’s goal is to manipulate specific decisions of a ML system for potential benefit—for example, to avoid being sentenced by an ML-enhanced judge.

Recent work has focused mainly on *evasion* attacks [5, 41, 16, 48, 30, 11], which can induce a *targeted* misclassification on a specific sample. As illustrated in Figures 1a and 1b, these test time attacks work by mutating the target sample to push it across the model’s decision boundary, without altering the training process and the decision boundary. They are not applicable in situations where the adversary does not control the target sample—for example, when she aims to influence a malware detector to flag a benign app developed by a competitor. Prior research has also shown the feasibility of targeted *poisoning* attacks [29, 28]. As illustrated in Figure 1c, these attacks usually blend crafted instances into the training set to push the model’s boundary toward the target. In consequence, they enable misclassifications for instances that the adversary cannot modify.

Existing attacks appear to be very effective, and defensive attempts are usually short-lived as they are broken by the follow-up work [10]. However, in order to understand the actual security threat introduced by these attacks we must model the capabilities and limitations of realistic adversaries. Adversary models usually overestimate the capabilities of the attacker, and create an incomplete assessment of the actual security threat posed to real world applications. For example, test time attacks often assume white-box access to the victim classifier [11]. As most security critical ML systems use proprietary models [2], these attacks might not reflect actual capabilities of a potential adversary. Black-box attacks often consider weaker adversaries when investigating the *transferability* of an attack. Transferability implies that a successful attack conducted by an adversary locally—usually on a limited model—is also successful on the target model. Black-box attacks often investigate transferability in the case where the local and target models use different training algorithms [32]. In contrast, ML systems used in the industry often rely on feature secrecy of their models, rather than algorithmic secrecy—for example, incorporating undisclosed features obtained

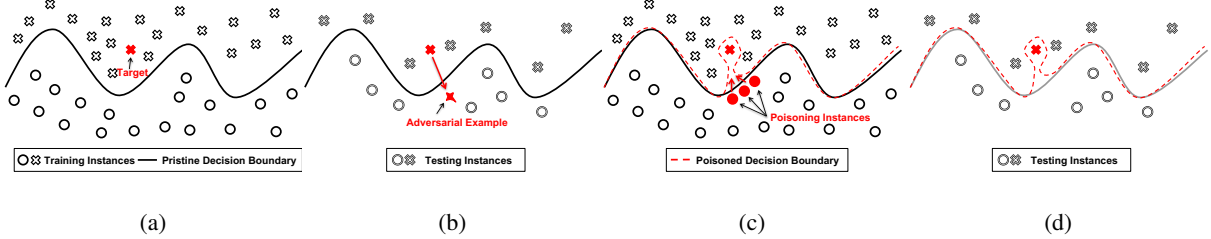


Figure 1: Targeted attacks against machine learning classifiers. (a) The pristine classifier would correctly classify the target. (b) An evasion attack would modify the target to cross the decision boundary. (c) Correctly labeled poisoning instances change the learned decision boundary. (d) At testing time, the target is misclassified but other instances are correctly classified.

using a known reputation score algorithm for malware detection [12].

In this paper we attempt to fill this gap and make a first step towards modeling realistic adversaries who aim to conduct attacks against ML systems. To this end, we propose the **FAIL** model, a general framework for analysis of ML attacks in settings with variable amount of adversarial knowledge and control over the victim, along four tunable dimensions: **F**eatures, **A**lgorithms, **I**nstances and **L**everage. By preventing any implicit assumptions about the adversarial capabilities, the model is able to accurately highlight the success rate of a wide range of attacks in realistic scenarios, and forms a common ground for modeling adversaries. Furthermore, the **FAIL** framework generalizes the transferability of attacks by providing a multidimensional basis for surrogate models. This provides insights into the constraints of realistic adversaries, which could be explored in future research on defenses against these attacks. For example, our evaluation suggests that crafting transferable samples with an existing evasion attack is more challenging than previously believed.

By taking into account the goals, capabilities and limitations of realistic adversaries, we also design **StingRay**, a targeted poisoning attack that can be applied to a broad range of settings. **StingRay** crafts *individually inconspicuous* samples that collectively push the model’s boundary toward a target instance while remaining *collectively inconspicuous* and bounding the collateral damage on the victim (Figure 1d). The instances that **StingRay** crafts are able to bypass three anti-poisoning defenses, including one that we adapted to account for targeted attacks. Furthermore, the poison samples are also *label agnostic*, being very similar to the existing training instances, and allowing the adversary to guess their likely label. Moreover, the **StingRay** attack is *model agnostic*: we describe concrete implementations against 4 ML systems, which use 3 different classification algorithms (Convolutional Neural Network, linear SVM and Random Forest). By subjecting **StingRay** to the **FAIL** analysis, we obtain insights into the *transferability of poison samples* across models, and highlight the most promising leads towards

future defenses against the threat.

In summary, this paper makes three contributions:

- We introduce the **FAIL** model, a general framework for modeling realistic adversaries and evaluating their impact. The model generalizes the transferability of attacks against ML systems, across various levels of adversarial knowledge and control. We show that a previous black-box evasion attack is less effective under generalized transferability.
- We propose **StingRay**, a targeted poisoning attack that overcomes the limitations of prior attacks. **StingRay** is effective against 4 real world classification tasks, even when launched by a range of weaker adversaries within the **FAIL** model. The attack also bypasses two existing anti-poisoning defenses.
- We systematically explore realistic adversarial scenarios and the effect of partial adversary knowledge and control on the resilience of ML models against a test-time attack and a training-time attack. Our results provide insights into the transferability of attacks across the **FAIL** dimensions and highlight potential directions for investigating defenses against these attacks.

This paper is organized as follows. In Section 2 we formalize the problem. In Section 3 we introduce our threat model and the **FAIL** attacker model. In Section 4 we describe the **StingRay** attack and its implementation. We present our experimental results in Section 5, review the related work in Section 6, and discuss the implications in Section 7.

2 Problem statement

Lack of a unifying adversary model that captures the dimensions of adversarial knowledge caused existing work to diverge in terms of adversary specifications. Prior work defined adversaries with inconsistent capabilities. For example, in [32] a *black-box* adversary possesses knowledge of the full feature representations, whereas its

counterpart in [48] has only access to the raw data (i.e. before feature extraction).

Compared to existing white-box or black-box models, in reality, things tend to be more nuanced. A commercial ML-based malware detector [2] can rely on a publicly known architecture with proprietary data collected from end hosts, and a mixture of known features (e.g. system calls of a binary), and undisclosed features (e.g. reputation scores of the binary). The existing adversary definitions are too rigid and cannot account for realistic adversaries against such applications. In this paper, we ask *how can we systematically model adversaries based on realistic assumptions about their capabilities?*

Some of the recent evasion attacks [25, 32] investigate the transferability property of their solutions. Proven transferability increases the strength of an attack as it allows adversaries with limited knowledge or access to the victim system to craft effective instances. Furthermore, transferability hinders defense strategies as it renders secrecy ineffective. However, existing work generally investigates transferability under single dimensions (e.g. limiting the adversarial knowledge about the victim algorithm). This weak notion of transferability limits the understanding of realistic attack capabilities on real systems and fails to shed light on potential avenues for defenses. In this paper we aim to provide a means to define and evaluate a more *general transferability*, across a wide range of adversary models.

Through our generalized view of the threat models, we observe limitations in existing training-time attacks. Existing attacks [49, 26, 18] often assume full control over the training process of classifiers, and have similar shortcomings to white-box attacks. Those that do not require full control usually omit important limitations of realistic adversaries. Targeted poisoning attacks [29, 28] require control of the labeling process, whereas the adversary is often unable to determine the labels assigned to the poison samples in the training set —consider a case where a malware creator may provide a poison sample for the training set of a ML-based malware detector, but its malicious/benign label will be assigned by the engineers who train the detector. These attacks risk being detected by existing defenses as they might craft samples that stand out from the rest of the training set. Moreover, they also risk causing collateral damage to the classifier; for example, in Figure 1c the attack can trigger the misclassification of additional samples from the target’s true class if the boundary is not moulded to include only the target. Such collateral damage reduces the trust in the classifier’s predictions, and thus the potential impact of the attack. Therefore, we aim to observe whether an attack could address these limitations and discover *how realistic is the targeted poisoning threat?*

Machine learning background. For our purposes, a *classifier* (or hypothesis) is a function $h : \mathcal{X} \rightarrow \mathcal{Y}$ that maps instances to labels to perform *classification*. An *instance* $\mathbf{x} \in \mathcal{X}$ is an entity (e.g., a binary program) that must receive a *label* $y \in \mathcal{Y} = \{y_0, y_1, \dots, y_n\}$ (e.g., reflecting whether the binary is malicious). We represent an instance as a vector $\mathbf{x} = (x_1, \dots, x_n)$ in an n -dimensional feature space \mathcal{X} , where the features reflect attributes of the artifact (e.g. APIs invoked by the binary). A function $D(\mathbf{x}, \mathbf{x}')$ represents the distance in the feature space between two instances $\mathbf{x}, \mathbf{x}' \in \mathcal{X}$. The function h can be viewed as a separator between the malicious and benign classes in the feature space \mathcal{X} ; the plane of separation between classes is called *decision boundary*. The *training set* $S \subset \mathcal{X}$ includes instances that have known labels $Y_S \subset \mathcal{Y}$. The labels for instances in S are assigned using an *oracle* — for a malware classifier, an oracle could be an antivirus service such as VirusTotal whereas for an image classifier, it might be a human annotator. The *testing set* $T \subset \mathcal{X}$ includes instances for which the labels are unknown to the learning algorithm.

The hypothesis space \mathcal{H} represents the set of possible hypotheses. An example of a hypothesis space is the class of linear classifiers, which label instances using a linear combination of the input vectors. A *learning algorithm* A aims to discover a mapping $h \in \mathcal{H}$ that minimizes the true error (the number of *mispredictions* $h(\mathbf{x}) \neq y$ for any $\mathbf{x} \in \mathcal{X}$ and its corresponding label $y \in \mathcal{Y}$). Because the algorithm has access only to the training set, it tries to find the hypothesis $h = A(S)$ that yields a small number of mistakes on the training set. This error is encoded in a loss function L that quantifies the distance between the predictions and the true labels.

Threat model. We focus on *targeted poisoning attacks* against machine learning classifiers. In this setting we refer to the victim classifier as Alice, the owner of the target instance as Bob, and the attacker as Mallory. Bob and Mallory could also represent the same entity. Bob possesses an instance $\mathbf{t} \in T$ with label y_t , called the *target*, which will get classified by Alice. For example, Bob develops a benign application, and he ensures it is not flagged by an oracle antivirus such as VirusTotal. Bob’s expectation is that Alice would not flag the instance either. Indeed, the target would be correctly classified by Alice after learning a hypothesis using a pristine training set S^* (i.e. $h^* = A(S^*), h^*(\mathbf{t}) = y_t$). Mallory has partial knowledge of Alice’s classifier and read-only access to the target’s feature representation, but they do not control either \mathbf{t} or the natural label y_t , which is assigned by the oracle. Mallory pursues two goals. The *first goal* is to introduce a targeted misclassification on the target by deriving a training set S from S^* : $h = A(S), h(\mathbf{t}) = y_d$, where y_d is Mallory’s desired label for \mathbf{t} . On binary clas-

sification, this translates to causing a false positive (FP) or false negative (FN). An example of FP would be a benign email message that would be classified as spam, while a FN might be a malicious sample that is not detected. In a multiclass setting, Mallory causes the target to be labeled as a class of choice.

Mallory’s *second goal* is to minimize the the effect of the attack on Alice’s overall classification performance. To quantify this effect, we introduce the Performance Drop Ratio (PDR), a metric that reflects the performance hit suffered by a classifier after poisoning. PDR is defined as the the ratio between the errors of the poisoned classifier and that of the pristine classifier: $PDR = \frac{L_S(h)}{L_{S^*}(h^*)}$. The metric encodes the fact that for a low-error classifier, Mallory could afford a smaller performance drop before raising suspicions.

In our setting, we model adversaries whose goal is to maintain a *PDR* of at least 0.95.

3 Modeling Realistic Adversaries

Knowledge and Capabilities. Realistic adversaries conducting training time or testing time attacks are constrained by an imperfect *knowledge* about the model under attack and by limited *capabilities* in crafting adversarial samples. For an attack to be successful, the samples crafted under these conditions must transfer to the original model. We formalize the adversary’s strength in the **FAIL** attacker model, which describes the adversary’s knowledge and capabilities along 4 dimensions:

- Feature knowledge $F_k = \{i \in 1 \dots n : x_i \text{ is known}\}$: the subset of features known to the adversary.
- Algorithm knowledge A' : the learning algorithm that the adversary uses to craft poison samples.
- Instance knowledge S' : the labeled training instances available to the adversary.
- Leverage $F_m = \{i \in 1 \dots n : x_i \text{ is modifiable}\}$: the subset of features that the adversary can modify.

The **F** and **A** dimensions constrain the attacker’s understanding of the hypothesis space \mathcal{H} . Without knowing A , the attacker would have to select an alternative learning algorithm A' and hope that the evasion or poison samples crafted for models created by A' transfer to models from A . Similarly, if some features are unknown (i.e., partial feature knowledge), the model that the adversary uses for crafting instances is an approximation of the original classifier. For classifiers that learn a representation of the input features (such as neural networks), limiting the **F** dimension results in a different,

approximate internal representation that will affect the success rate of the attack. These limitations result in an inaccurate *assessment* of the impact that the crafted instances will have, and affect the success rate of the attack. The **I** dimension affects the accuracy of the adversary’s view of the instance space. As S' might be a subset or an approximation of S^* , the poisoning and evasion samples might exploit gaps in the instance space that are not present in the victim’s model. This, in turn, could lead to an impact overestimation on the attacker side. Finally, the **L** dimension affects the adversary’s *ability* to craft attack instances. The set of modifiable features restricts the regions of the feature space where the crafted instances could lie. For poisoning attacks this places an upper bound on the ability of samples to shift the decision boundary while for evasion it could affect their effectiveness. The unmodifiable features can, in some cases, cancel out the effect of the modified ones. An adversary with partial leverage needs extra effort, e.g. to craft more instances (for poisoning) or to attack more of the modifiable features (for both poisoning and evasion).

The **FAIL** model generalizes the transferability property. The prior work on transferability [32] focused on the **A** dimension, and only in the context of evasion attacks. This may not be the most important dimension in practice, however. ML-based systems employed in the security industry [19, 12, 42, 35, 13] often rely on undisclosed features to render attacks more difficult. The resilience against adversaries with partial knowledge along the **F** dimension has not been evaluated systematically, and the transferability of poison samples is an open question.

Constraints. The attacker’s strategy is also influenced by a set of *constraints* that drive the attack design and implementation. While these are attack-dependent, we broadly classify them into three categories: *success*, *defense* and *budget* constraints. *Success* constraints encode the attacker’s goals and considerations that directly affect the effectiveness of the attack, such as the assessment of the target instance classification. *Defense* constraints refer to the attack characteristics meant to circumvent existing defenses (e.g. the post-attack performance drop on the victim). *Budget* considerations address the limitations in an attacker’s resources, such as the maximum number of crafted instances or, for poisoning attacks, the maximum number of queries to the victim model.

Implementing the FAIL dimensions. Performing empirical evaluations within the **FAIL** model requires further design choices that depend on the application domain and on the attack surface of the system. To simulate weaker adversaries systematically, we formulate a questionnaire to guide the design of experiments focusing on each dimension of our model.

For the **F** dimension, we ask: *What features could be kept secret? Could the attacker access the exact feature values?* Feature subsets may not be publicly available (e.g. derived using a proprietary malware analysis tool, such as dynamic analysis in a contained environment), or they might be directly defined from instances not available to the attacker (e.g. low frequency word features). Similarly, the exact feature values could be secret, e.g. because of defensive feature squeezing [47] or because features are learned representations of the input features (e.g. neural networks).

The questions related to the **A** dimension are: *Is the algorithm class known? Is the training algorithm secret? Are the classifier parameters secret?* These questions define the spectrum for adversarial knowledge with respect to the learning algorithm: black-box access, if information is public, gray-box, where the attacker has partial information about the algorithm class or the ensemble architecture, or white-box, for complete adversarial knowledge.

The **I** dimension controls the overlap between the instances available to the attacker and those used by the victim. Thus, here we ask: *Is the entire training set known? Is the training set partially known? Are the instances known to the attacker sufficient to train a robust classifier?* An applications might use instances from the public domain (e.g. a vulnerability exploit predictor) and the attacker could leverage them to the full extent in order to derive their attack strategy. However, some applications, such as a malware detector, might rely on private or scarce instances that limit the attacker’s knowledge of the instance space. The scarcity of these instances drives the robustness of the attacker classifier which in turn defines the perceived attack effectiveness.

The **L** dimension encodes the practical capabilities of the attacker when crafting attack samples. Here we ask: *Which features are modifiable by the attacker?* For some applications, the attacker may not be able to modify certain types of features, either because she does not control the generating process (e.g. an exploit predictor that gathers features from multiple vulnerability databases) or when the modifications would compromise the instance integrity (e.g. a watermark on images that prevents the attacker from modifying certain features).

4 The StingRay Attack

In this section we introduce the StingRay attack, which achieves targeted poisoning while preserving overall classification performance. StingRay is a general framework for crafting poison samples.

At a high level, our attack builds a set of poison instances by starting from base instances that are close to the target in the feature space but are labeled as the de-

Algorithm 1 The StingRay attack.

```

1: procedure CRAFTATTACKINSTANCES( $S', Y_{S'}, \mathbf{t}, y_t, y_d$ )
2:    $I = \emptyset$ 
3:    $h = A'(S')$ 
4:   repeat
5:      $\mathbf{x}_b = \text{GETBASEINSTANCE}(S', Y_{S'}, \mathbf{t}, y_t, y_d)$ 
6:      $\mathbf{x}_c = \text{CRAFTINSTANCE}(\mathbf{x}_b, \mathbf{t}, F_a, s(\cdot, \cdot))$ 
7:      $NI = L_{S'} \cup \{\mathbf{x}_c\} - L_{S'}$ 
8:     if  $NI < \delta_{NI}$  then
9:        $I = I \cup \{\mathbf{x}_c\}$ 
10:       $h = A'(S' \cup I)$ 
11:    until  $(|I| > N \text{ and } h(\mathbf{t}) = y_d) \text{ or } |I| > M_I$ 
12:     $PDR = \text{GETPDR}(S', Y_{S'}, I, y_d)$ 
13:    if  $h(\mathbf{t}) \neq y_d$  or  $PDR < \delta_{PDR}$  then
14:      return  $\emptyset$ 
15:    return  $I$ 
16: procedure GETBASEINSTANCE( $S', Y_{S'}, \mathbf{t}, y_t, y_d$ )
17:   for  $\mathbf{x}_b, y_b$  in  $\text{SHUFFLE}(S', Y_{S'})$  do
18:     if  $D(\mathbf{t}, \mathbf{x}_b) < \delta_D \text{ and } y_b = y_d$  then
19:       return  $\mathbf{x}_b$ 

```

sired target label y_d , as illustrated in the example from Figure 2. In this example, the adversary has created a malicious Android app \mathbf{t} , which includes suspicious features (e.g. the `WRITE_CONTACTS` permission on the left side of the figure), and she wishes to prevent a malware detector from flagging this app. The adversary therefore selects a benign app \mathbf{x}_b as a base instance. To craft each poison instance, StingRay alters a subset of a base instance’s features so that they resemble those of the target. As shown on the right side of Figure 2, these are not necessarily the most suspicious features, so that the crafted instance will likely be considered benign. Finally, StingRay filters crafted instances based on their negative impact on instances from S' , ensuring that their individual effect on the target classification performance is negligible. We repeat the sample crafting procedure until there are enough instances to trigger the misclassification of \mathbf{t} . Algorithm 1 shows the pseudocode of the attack’s two general-purpose procedures.

We describe concrete implementations of our attack against four existing applications: an image recognition system, an Android malware detector, a Twitter-based exploit predictor, and a data breach predictor. We reimplement the systems that are not publicly available, using the original classification algorithms and the original training sets to reproduce those systems as closely as possible. In total, our applications utilize three classification algorithms—convolutional neural network, linear SVM and random forest—that have distinct characteristics.

This spectrum illustrates the first challenge for our

attack: identifying and encapsulating the application-specific steps in StingRay, to adopt a modular design with broad applicability. Making poisoning attacks practical raises additional challenges. For example, a naïve approach would be to inject the target with the desired label into the training set: $h(\mathbf{t}) = y_d$ (**S.I**). However, this is impractical because the adversary, under our threat model, does not control the labeling function. Therefore, **GETBASEINSTANCE** works by selecting instances \mathbf{x}_b that already have the desired label and are close to the target in the feature space (**S.II**).

A more sophisticated approach would mutate these samples and use poison instances to push the model boundary toward the target’s class [28]. However, these instances might resemble the target class too much, and they might not receive the desired label from the oracle or even get flagged by an outlier detector. In **CRAFTINSTANCE**, we apply tiny perturbations to the instances (**D.III**) and by checking the negative impact NI of crafted poisoning instances on the classifier (**D.IV**) we ensure they remain *individually inconspicuous*.

Mutating these instances with respect to the target [29] (as illustrated in Figure 1c) may still reduce the overall performance of the classifier (e.g. by causing the misclassification of additional samples similar to the target). We overcome this via **GETPDR** by checking the performance drop of the attack samples (**S.V**), therefore ensuring that they remain *collectively inconspicuous*.

Even so, the StingRay attack adds robustness to the poison instances by crafting more instances than necessary, to overcome sampling-based defenses (**D.VI**). Nevertheless, the attack has a sampling budget that dictates the allowable number of crafted instances (**B.VII**). A detailed description of StingRay is found in Appendix A.

Attack Constraints. The attack presented above has a series of constraints that shape its effectiveness. Reasoning about them allows the adaptation of the attack guidelines to the specific constraints of each application. These span all three categories identified in Section 3: Success(**S.**), Defense(**D.**) and Budget(**B.**):

- S.I** $h(\mathbf{t}) = y_d$: the desired class label for target
- S.II** $D(\mathbf{t}, \mathbf{x}_b) < \delta_D$: the inter-instance distance metric
- D.III** $F_a = \frac{1}{|I|} \sum s(\mathbf{x}_c, \mathbf{t})$ for all $\mathbf{x}_c \in I$, where $s(\cdot, \cdot)$ is a *similarity* metric: crafting target resemblance
- D.IV** $NI < \delta_{NI}$: negative impact of poisoning instances
- S.V** $PDR < \delta_{PDR}$: the perceived performance drop
- D.VI** $|I| \geq N$: the minimum number of poison instances
- B.VII** $M_I = |I|$: maximum number of poisoning instances

The perceived success on the attacker goals (**S.I** and **S.V**) dictate whether the attack is triggered. If the *PDR* is large, the attack might become indiscriminate and the risk of degrading the overall classifier’s performance is high. The actual *PDR* could only be computed in the white-box setting. For scenarios with partial knowledge, it is approximated through the perceived *PDR* on the available classifier.

The impact of crafted instances is influenced by the distance metric and the feature space used to measure instance similarity (**S.II**). For applications that learn feature representations (e.g. neural nets), the similarity of learned features might be a better choice for minimizing the crafting effort.

The set of features that are actively modified by the attacker in the crafted instances (**D.III**) defines the *target resemblance* for the attacker, which imposes a trade-off between their inconspicuousness and the effectiveness of the sample. If this quantity is small, the crafted instances are less likely to be perceived as outliers, but a larger number of them is required to trigger the attack. A higher resemblance could also cause the oracle to assign crafted instances a different label than the one desired by the attacker.

The loss difference of a classifier trained with and without a crafted instance (**D.IV**) approximates the negative impact of that instance on the classifier. It may be easy for an attacker to craft instances with a high negative impact, but these instances may also be easy to detect using existing defenses.

In practice, the cost of injecting instances in the training set can be high (e.g. controlling a network of bots in order to send fake tweets) so the attacker aims to minimize the number of poison instances (**D.VI**) used in the attack. The adversary might also discard crafted instances that do not have the desired impact on the ML model. Additionally, some poison instances might be filtered before being ingested by the victim classifier. However, if the number of crafted instances falls below a threshold N , the attack will not succeed.

The maximum number of instances that can be crafted (**B.VII**) influences the outcome of the attack. If the attacker is unable to find sufficient poison samples after crafting M_I instances, they might conclude that the large fraction of poison instances in the training set would trigger suspicions or that they used their available crafting budget.

Delivering Poisoning Instances. The mechanism through which poisoning instances are delivered to the victim classifier is dictated by the application characteristics and the adversarial knowledge. In the most general scenario, the attacker injects the crafted instances alongside existing ones, expecting that the victim classifier

Layer Type	Layer size
Convolution + ReLU	$3 \times 3 \times 32$
Convolution + ReLU	$3 \times 3 \times 64$
Max Pooling	2×2
Dropout	0.25
Convolution + ReLU	$3 \times 3 \times 128$
Max Pooling	2×2
Convolution + ReLU	$3 \times 3 \times 128$
Max Pooling	2×2
Dropout	0.25
Fully Connected + ReLU	1024
Dropout	0.5
Softmax	10

Table 1: The architecture of our NN-based image classifier.

Parameter	Value
Optimizer	ADAM
Learning Rate	0.0009
Decay	0.000001
Batch Size	32
Epochs	25

Table 2: The parameters of our NN-based image classifier.

will be trained on them. For applications where models are updated over time or trained in mini-batches (such as an image classifier based on neural networks), the attacker only requires control over a subset of such batches and might choose to deliver poison instances through them. Finally, in cases where the attacker is unable to create new instances (such as a vulnerability exploit predictor), she will rely on modifying the features of exiting ones by poisoning the feature extraction process. The applications used to showcase StingRay will all highlight these scenarios and the design considerations driving the attack.

4.1 Attack implementation

Image classification. We first poison a neural-network (NN) based application for image classification, often used for demonstrating evasion attacks in the prior work. The input instances are images and the labels correspond to objects that are depicted in the image (e.g. airplane, dog, ship). We evaluate StingRay on our own implementation for CIFAR-10 [22], a dataset of 60,000 RGB images of 32x32 pixels split into 10 classes. 50,000 of these images are used for training, while the remaining ones are left for validation and testing. In this scenario, the attacker has an image \mathbf{t} with true label y_t (e.g. a dog) and wishes to trick the model into classifying it as a specific class y_d (e.g. a cat).

We implement a convolutional neural network, architecture that achieves 78% accuracy on the CIFAR task, which is comparable to other studies [34, 11]. Our network uses convolutional, max pooling, and dropout layers. The exact architecture, presented as a stack of layers, is listed in Table 1. For training, we used an ADAM optimizer with parameters listed in Table 2.

Once the network is trained on the benign inputs, we proceed to poison the classifier. We first generate poison instances and group them into batches alongside benign inputs. We define $\gamma \in [0, 1]$ to be the *mixing parameter* which controls the amount of poison instances in a batch. In our experiments we varied γ over $\{0.125, 0.5, 1.0\}$ (i.e. 4, 16, and 32 instances of the batch are poisonous) and always selected the value that provided the best attack success rate¹. We then update² the previously trained network using these batches until either the network is successfully poisoned, or we exceed the number of available poisoning instances, dictated by the cut-off threshold M_I . It is worth noting that if the learning rate is high and the batch contains too many poison instances, the attack could become indiscriminate. Conversely, too few crafted instances would not succeed in changing the target prediction, so the attacker needs to control more batches.

The main insight that motivates our method for generating adversarial samples is that there exist inputs to a network $\mathbf{x}_1, \mathbf{x}_2$ whose distance in pixel space $\|\mathbf{x}_1 - \mathbf{x}_2\|$ is much smaller than their distance in deep feature space $\|H_i(\mathbf{x}_1) - H_i(\mathbf{x}_2)\|$, where $H_i(\mathbf{x})$ is the value of the i 'th hidden layer's activation for the input \mathbf{x} , for some i . This insight is motivated by the very existence of test-time adversarial examples, where inputs to the classifier are very similar in pixel space, but are successfully misclassified by the neural network [5, 41, 16, 48, 30, 11]. Our attack consists of selecting *base* instances that are close to the target \mathbf{t} in *deep feature space*, but are labeled by the oracle as the attacker's desired label y_d . The instances are then perturbed such that the *distance to the target* \mathbf{t} in deep feature space is minimized and the resulting adversarial image is within δ_D distance in pixel space to \mathbf{t} . In our experiments, we chose the deep feature space to be represented by $H_3(\cdot)$, the activations of the 3'rd hidden layer. This choice is a result of the *transferability-perturbation* trade-off induced by the used deep feature space: selecting a lower layer in the network provides better transferability [50] of the poison instances, at the cost of increased incurred perturbation, while selecting a higher-level layer may enable instances with low perturbation in lieu of transferability.

To generate the poison instances, we modified the

¹ We kept the value of γ fixed across successive updates.

² The update is performed on the entire network (i.e. all layers are updated).

JSMA method for evasion attacks proposed in [31]. Although StingRay could technically employ any evasion attack, we picked JSMA due to its proven transferability in evasion scenarios [33]. In JSMA, adversarial samples are generated by perturbing pairs of pixels that most increase the classification output for the attacker’s target class or decrease the output for the other classes. This is achieved by using a *Saliency Map*, which quantifies, for each input pixel, this change in the output of the network. The Saliency Map makes use of the *Jacobian* of the function $\mathbf{F}(\cdot)$ learned by network and is expressed as:

$$\nabla \mathbf{F}(\mathbf{x}) = \frac{\partial \mathbf{F}(\mathbf{x})}{\partial \mathbf{x}}$$

Since our objective is to minimize the deep feature distance between the input \mathbf{x} and the target \mathbf{t} , we replace the Saliency Map with the *Gradient* of the deep feature distance w.r.t. the input image. We can formally describe the value of the saliency map for a specific input pixel j and a *fixed* target \mathbf{t} as:

$$S_{\mathbf{t}}(\mathbf{x})[j] = \frac{\partial ||H_i(\mathbf{t}) - H_i(\mathbf{x})||_2}{\partial x_j}$$

Using this formulation of the Saliency Map, we employ the optimization procedure of JSMA.

We pick 100 target instances uniformly distributed across the class labels. The desired label y_d is the one closest to the true label y_t from the *attacker’s classifier* point of view (i.e. it is the second best guess of the classifier). We set the cut-off threshold $M_I = 64$, equivalent to two mini-batches of 32 examples. The perturbation is upper-bounded at $\delta_D < 3.5\%$ resulting in a target resemblance $||F_a|| < 110$ pixels. We run a poisoning attack for each one of the 100 target instances and report the results as averages across these runs.

Android malware detection. The Drebin Android malware detector [3] uses a linear SVM classifier to predict if an app is malicious or benign. The Drebin dataset [3] consists of 123,453 Android apps, including 5,560 malware samples. These apps were labeled using 10 AV engines on VirusTotal [46], considering that apps with at least two detections are malicious. The feature space has 545,333 dimensions. We use stratified sampling and split the dataset into 60%-40% folds training and testing respectively, reproduce to mimic the original classifier. The features are extracted from the application archives (APKs) using two techniques. First, from the *AndroidManifest XML* file, which contains meta information about the app, the authors extract the permission requested, the application components and the registered system callbacks. Second, after disassembling the *dex* file, which contains the app bytecode, the system extracts suspicious Android framework calls, actual permission

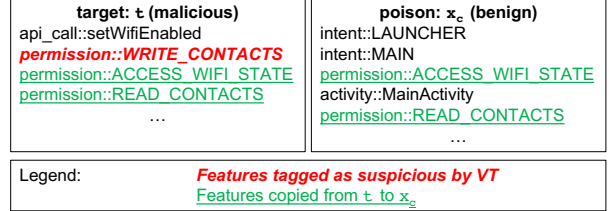


Figure 2: The sample crafting process illustrated for the Drebin Android malware detector. Suspicious features are emphasized in VirusTotal reports, but the attacker is not constrained to copying them.

usage and hardcoded URLs. The features are represented as bit vectors, where each index specifies whether the application contains the feature.

The adversary aims to misclassify an Android app \mathbf{t} . Although the problems of inducing a targeted false positive (FP) and a targeted false negative (FN) are analogous from the perspective of our definitions, in practice the adversary is likely more interested in targeted FNs, so we focus on this case in our experiments. We evaluate this attack by selecting target instances from the testing set that would be correctly labeled as malicious by the classifier. We then craft instances by adding active features (permissions, API calls, URL requests) from the target to existing benign instances, as illustrated in Figure 2. Each of the crafted apps will have a subset of the features of the \mathbf{t} app, to remain individually inconspicuous. The poisoning instances are mixed with the pristine ones and used to train the victim classifier from scratch.

We craft 1,717 attacks to test the attack on the Drebin classifier. We use a cutoff threshold $M_I = 425$, which corresponds to 0.5% of the training set. The base instances are selected using the Manhattan distance D_1 and each poisoning instance has a target resemblance of $||F_a|| = 10$ features and a negative impact $\delta_{NI} < 50\%$.

Twitter-based exploit prediction. In [39], the authors present a system, based on a linear SVM, that predicts which vulnerabilities are going to be exploited using features extracted from Twitter and public vulnerability databases. For each vulnerability, the predictor extracts word-based features (e.g. the number of tweets containing the word *code*), Twitter statistics (e.g. number of distinct users that tweeted about it), and domain-specific features for the vulnerability (e.g. CVSS score). The dataset contains 4,140 instances out of which 268 are labeled as positive (a proof-of-concept exploit is publicly available). The classifier uses 72 features from 4 categories: CVSS Score, Vulnerability Database, Twitter traffic and Twitter word features. Due to the class imbalance, we use stratified samples of 60%-40% of the dataset for training and testing respectively.

In this case, the adversary has developed a new exploit \mathbf{t} for a disclosed vulnerability, and plans to utilize it

while also evading the classifier. However, the adversary would like to evade the Twitter-based detector, to prevent potential victims from receiving an early warning about the exploitation attempts.

Because Twitter is a free and open service, the adversary may post tweets, may utilize multiple accounts to emulate trending topics and may utilize underground services to acquire followers and trigger retweets. However, the adversary is unable to prevent other users who observe the exploit from tweeting or to alter the vulnerability details recorded in the public vulnerability databases. In consequence, the adversary cannot introduce new instances in the training set—unlike for the Android malware detector or the image classifier—as the vulnerabilities classified come from the vulnerability databases. Instead, the attacker can post tweets that alter some features of vulnerabilities already included in the training set.

The targeted attack consists of choosing a set I of vulnerabilities that are similar to \mathbf{t} (e.g. same product or vulnerability category), have no known exploits and gathered fewer tweets, and posting crafted tweets about these vulnerabilities that include terms normally found in the tweets about the target vulnerability. In this manner, the classifier gradually learns that these terms indicate vulnerabilities that are not exploited. However, the attacker’s capabilities are somewhat limited since the features extracted from sources other than Twitter are not under the attacker’s control. In our experiments, we select target instances for which an exploit has been reported (at a later time) in the wild or released as a proof of concept. As part of the poisoning attack, we then choose vulnerabilities from the training set for which no known exploit has been reported. We then attempt to match \mathbf{t} ’s set of modifiable Twitter features (F_m), simulating an attacker who controls a network of accounts with well established statistics (e.g. number of followers). These accounts could originate either from black markets or compromised accounts [17, 43]. Our adversary uses these accounts to tweet about specific vulnerabilities. In our simulation, we inject users and their tweets containing targeted keywords in the dataset during the feature extraction process. Generating tweets as a sequence of keywords is sufficient to circumvent the unigram feature model embodied by this classifier. A more sophisticated adversary might apply natural language generation techniques [36] to further increase the chances that posts will be deemed legitimate.

We simulate 1,932 attacks setting $M_I = 20$ and selecting the CVEs to be poisoned using the Euclidean distance D_2 with $\delta_{NI} < 50\%$.

Data breach prediction. The fourth application we analyze is a data breach predictor proposed in [27]. The system attempts to predict whether an organization is

going to suffer a data breach, by using a Random Forest classifier. The features used in classification include indications of bad IT hygiene (e.g. misconfigured DNS servers) and malicious activity reports (e.g. blacklisting of IP addresses belonging to the organization). These features are absolute values (i.e. organization size), as well as timeseries-based statistics (e.g. duration of attacks). The Data Breach Investigations Reports (DBIR) [45] provides the ground truth. The classifier uses 2,292 instances with 382 positive-labeled examples. The 74 existing features are extracted from externally observable network misconfiguration symptoms as well as blacklisting information about hosts in an organization’s network. We use stratified sampling to build a training set containing 50% of the corpus and use the rest for testing and choosing targets for the attacks. A similar technique is used to compute the FICO Enterprise Security Score [15]. In this case, the adversary plans to hack an organization \mathbf{t} , but wants to avoid triggering an incident prediction despite the eventual blacklisting of the organization’s IPs. To achieve their goal, the adversary chooses a set I of organizations that do not appear in the DBIR and modifies their feature representation. For example, the adversary could initiate malicious activities (e.g. exploitation, spam) that appear to originate from these organizations or could hack the organizations and use their servers with the sole purpose of getting them blacklisted. We again assume that some of the features cannot be modified (e.g. the size of the network), while others (e.g. the blacklisting of hosts) can be manipulated indirectly through malicious activity. This gradually forces the classifier to reduce the weight of features that the adversary cannot manipulate. In our experiments, the attacker has limited Leverage and is only able to influence timeseries-based features indirectly, by injecting information in various blacklists. In practice, this could be done by either compromising the blacklists or hacking the organizations themselves in order to initiate the poisoning.

We generate 2,002 attacks under two scenarios: the attacker has compromised a blacklist and is able to influence the features of many organizations, or the attacker has infiltrated a few organizations and it uses them to modify their reputation on all the blacklists. We set $M_I = 50$ and the instances to be poisoned are selected using the Euclidean distance D_2 with $\delta_{NI} < 50\%$.

4.2 Bypassing Anti-Poisoning Defenses

In this section we discuss existing defenses against poisoning attacks and their limitations.

Micromodels. Micromodels defense was proposed for cleaning training data for network intrusion de-

tectors [14]. The defense trains classifiers on non-overlapping epochs of the training set (*micromodels*) and evaluates them on the training set. By using a majority voting of the micromodels, training instances are marked as either safe or suspicious. Intuition is that attacks have relatively low duration and they could only affect a few micromodels. It also relies on the availability of accurate instance timestamps.

Reject on Negative Impact (RONI). RONI defense was proposed against spam filter poisoning attacks [4]. RONI measures the incremental effect of each individual suspicious training instance and discards the ones with a relatively significant negative impact on the overall performance. RONI sets a threshold by observing the average negative impact of each instance in the training set, and marks an instance when its performance impact exceeds the threshold. The threshold determines RONI’s ultimate effectiveness, the number of instances marked and the precision of detecting poison samples. In consequence, RONI assumes a clean set for an accurate threshold. For scenarios like ours with no initially clean set, we implemented an iterative RONI variant, as suggested in [40] that iterates over a set of threshold values instead of measuring a single threshold. RONI is computationally inefficient as the number of trained classifiers scales by the number of instances in the training set. To the best of our knowledge, this version has not been implemented and evaluated before.

Target aware RONI (tRONI). RONI fails to mitigate *targeted* attacks [29] because the poison instances might not cause a significant performance drop individually. We develop a targeted RONI variant that incorporates the knowledge of a test time misclassification to determine responsible training instances. Unlike RONI, which gauges instance negative impact on a set of instances, tRONI only considers classification of the target instance. In consequence, tRONI identifies instances that distort the target classification significantly. Moreover, there exists an arms race between an attacker aware of the negative impact of poison instances (Cost **D.V**) and the thresholds used by tRONI, as described in Appendix B.

Algorithm 2 describes the targeted RONI algorithm. The **ITERATIVE TARGETED RONI** procedure takes as input the base training set (S, Y_S) , the target instance of the adversary and its true label (x_T, Y_{x_T}) , a list of significance threshold values THS , in decreasing order,³ the number of subsets sampled from the training set N , and the size of these subsets K . We use the RI list to keep track of the training instances that the algorithm rejects. At the end of $|THS|$ iterations, the algorithm returns RI .

³The threshold values decrease to make the algorithm less selective about rejections, as the training set becomes cleaner.

Algorithm 2 Targeted RONI algorithm.

```

1: procedure TARGETEDRONI
2:    $(S, Y_S, x_T, Y_{x_T}, THS, N, K)$ 
3:    $RI = []$ 
4:   for all  $TH$  in  $THS$  do
5:     for all  $(x, Y_x) \in (S, Y_S)$  do
6:       if  $x \in RI$  then
7:         continue
8:        $TS, Y_{TS} = \text{GENSUBSETS}(S, Y_S, x_T, Y_{x_T}, N, K, RI)$ 
9:        $R = \text{QUERYINSTANCE}(TS, Y_{TS}, x, Y_x, x_T, Y_{x_T})$ 
10:      if  $\text{REJECTINSTANCE}(R, Y_Q, TH)$  then
11:         $RI.append(I)$ 
12:   return  $RI$ 

```

For THS , we utilize the gradual cleaning idea that gradually lowers the allowed negative impact threshold of current iteration for rejecting instances. Thus, THS is a decreasingly sorted list of thresholds that aims to reject the instances ranging from obviously negatively impactful to subtly negatively impactful.

The **GENSUBSETS** procedure samples N subsets from the (S, Y_S) , each with K training instances, without using the instances in RI , which have already been discarded. The procedure ensures that the classifiers trained on these subsets produce the correct label Y_{x_T} for the target instance x_T . The procedure returns these sampled subsets and the corresponding labels, (TS, Y_{TS}) . Experimentally, we found out that K should be low enough to allow the instances to have significant impact on the classifiers trained on the subsets, which makes distinguishing the reliable training instances from the unreliable ones.

The **QUERYINSTANCE** procedure takes these subsets, adds the current training instance (x, Y_x) to each one, and trains N new classifiers. The procedure then tests these classifiers on the target instance, (x_T, Y_{x_T}) , and returns the classification results of the classifiers as a list of labels, R . The **REJECTINSTANCE** procedure, takes these results, the correct label of the target instance Y_{x_T} , and the significance threshold of current iteration TS . The procedure returns *true* if the ratio of mispredictions for the target instance (determined using R) to the number of classifiers N exceeds the significance value of the current iteration, TS . In this case, we reject the current instance (x, Y_x) .

Because the RONI variants examine training instances one by one, the order in which we iterate over the S set may influence the algorithms’ effectiveness. We randomize this order to avoid additional assumptions about the training set, and also to avoid the circumstances that might be originated from the initial ordering of the data set.

Moreover, adversarial samples that have a small *individual* impact by that trigger mispredictions when *collectively* used in the training process—such as the ones

crafted by StingRay—may evade both RONI variants.

All these defenses aim to increase the attacker costs by forcing her to craft instances that result in a small loss difference (Cost **D.IV**). Therefore, they assume that the poison instances stand out from the rest, and they affect the classifier. An attack, such as StingRay, exploits this assumption to evade detection by crafting a small number of inconspicuous poison samples.

4.3 Labeling poisoning instances

Although the attacker could craft poisoning instances that closely resemble of the target, the oracle that labels these instances is outside their control. If the poisoning instances are not inconspicuous, they could be flagged as outliers or the oracle could assign them a label that is not beneficial for the attack. It is therefore beneficial to reason about the oracles specific to all applications and the considerations for crafted instances to get the desired label.

For the image classifier, the most common oracle is a consensus of human analysts. In an attempt to map the effect of adversarial perturbations on human perception, in [31], the authors found through a user study that the maximum fraction of perturbed pixels at which humans will correctly label an image is 14%. We therefore designed our experiments to remain within these bounds. In the StingRay implementation, we measured the pixel space perturbation δ_D as the l_∞ distance and discard poison samples with $\delta_D > 0.14$ prior to adding them to I .

The Drebin classifier uses VirusTotal as the oracle. To ensure that our crafted apps would indeed be considered benign, we query VirusTotal [46] and we utilize the same method as Drebin for labeling samples as malicious or benign. To modify selected features of the Android apps, we reverse-engineer Drebin’s feature extraction process to generate apps that would have the desired feature representation. We systematically generate these applications for the scenario where only the subset of features extracted from the *AndroidManifest* are modifiable by the attacker. Specifically, we start from the source code of benign applications and add nodes to the XML (e.g. new permissions) that were extracted from the target application. We then repack these applications and submit them to VirusTotal for labeling. We aimed to craft 25,482 applications corresponding to 549 targets. Due to inconsistencies between the feature names and the *AndroidManifest* nodes, we were unable to generate valid *apk* files in 5,850 of these cases. We then submitted the remaining 19,632 files to VirusTotal and measured their detection rate as per the Drebin paper. For 7,785 labeled benign in the Drebin ground truth, VirusTotal returned malicious labels. This is likely because antivirus products have started detecting them after the Drebin ground truth

was labeled; incorrect labels in Drebin were also reported in prior work [52]. For the 11,847 benign-labeled base instances, 1,311 of their crafted instances were detected, while 10,536 passed through. The number of crafted instances that were detected may decrease if the attacker adds fewer features to base instances (in this case, we added 10 features per instance). However, the 89% success rate suggests that this attack is practical.

For the exploit and databreach predictors, the labeling is done independently of the feature representations used by these two systems. Therefore the attacker has more degrees of freedom in modifying the features of instances in I , knowing that the desired labels will be preserved. For the exploit predictor, the attacker manipulates the public discourse around existing vulnerabilities, but the labeling is done with respect to the existence of an exploit. The desired label of instances in I is inherently maintained. In case of the databreach predictor, the attacker targets organizations with no known breach, and aims to poison the blacklists that measure their hygiene. The attacker does not necessarily require access to the organization networks and the labeling entity (DBIR).

5 Evaluation

We start by evaluating the effectiveness of existing defenses against StingRay (Section 5.1). We consider the strongest (white-box) adversary to determine upper bounds for the resilience against attacks, without assuming any degree of secrecy. We then evaluate weaker adversaries, within the **FAIL** model, on the image and malware classifiers (Section 5.2).

Our evaluation seeks to answer four research questions: *Is StingRay effective against multiple applications and defenses?* *What are the limitations of realistic poisoning adversaries?* *Are targeted poison samples transferable?* *Could we evaluate the transferability of existing evasion attacks?*

We quantify the effectiveness of StingRay using two metrics: the percentage of successful attacks (SR) and the performance drop ratio (PDR). We measure the PDR on heldout testing sets by considering either the average accuracy, on applications with balanced data sets, or the F1 score (the harmonic mean between precision and recall), which is more appropriate for highly imbalanced data sets.

5.1 Effectiveness of the StingRay attack

Table 3 explores the effectiveness of StingRay and compares existing defense mechanisms in terms of their ability to prevent the targeted mispredictions.

Image classifier. We observe that the attack is successful in 70% of the cases and yields an average PDR of

	StingRay	RONI	tRONI	MM
	$ I /SR\%/PDR$	Fix\%/PDR		
Images	16/70/0.97	-/-	-/-	-/-
Malware	77/50/0.99	0/0.98	15/0.98	-/-
Exploits	7/6/1.00	0/0.97	40/0.67	0/0.33
Breach	18/34/0.98	-/-	20/0.96	55/0.91

Table 3: Effectiveness of StingRay and of existing defenses against it on all applications. Each attack cell reports the average number of poison instances $|I|$, the success rate (SR) and actual PDR. Each defense cell reports the percentage of fixed attacks and the PDR after applying it.

0.97, requiring an average of 16 instances. Upon further analysis, we discovered that the performance drop is due to other testing instances similar to the target being misclassified as y_d . By tuning the attack parameters (e.g. the layer used for comparing features, the degree of allowed perturbation) to generate poison instances that are more specific to the target, the performance drop on the victim could be further reduced at the expense of requiring more poisoning instances. Nevertheless, this shows that neural nets define a fine-grained boundary between class-targeted and instance-target poisoning attacks, and that it is not straightforward to discover it, even with complete adversarial knowledge.

None of the three poisoning defenses are applicable on this task. RONI and tRONI require training over 50,000 classifiers for each level of inspected negative impact. Training these models is prohibitive for neural networks which are known to be computationally intensive to train. Since we could not determine reliable timestamps for the images in the dataset, MM was not applicable either.

Malware classifier. StingRay succeeds in half of the cases and yields a negligible performance drop on the victim. The attack being cutoff by the crafting budget on most failures (Cost **M.VII**) suggests that some targets might be too "far" from the class separator and that moving this separator becomes difficult. Nevertheless, understanding what causes this hardness remains an open question.

On defenses, we observe that RONI often fails to build correctly-predicting folds on Drebin and times out. Hence, we investigate the defense against only 97 successful attacks for which RONI did not timeout. MM rejects all training instances while RONI fails to detect any attack instances. tRONI detects very few poison instances, fixing only 15% of attacks, as they do not have a large negative impact, individually, on the misclassification of the target. None of the existing defenses are able to fix a large fraction of the induced mispredictions.

Exploit predictor. While poisoning a small number of instances, the attack has a very low success rate. This is due to the fact that the non-Twitter features are not

modifiable; if the dataset does not contain other vulnerabilities similar to the target (e.g. similar product or type), the attack would need to poison more CVEs, reaching M_I before succeeding. The result, backed by our FAIL analysis of the other linear classifier in Section 5.2, highlights the benefits of built in Leverage limitations in protecting against such attacks.

MM correctly identifies the crafted instances but also marks a large fraction of positively-labeled instances as suspicious. Consequently, the PDR on the classifier is severely affected. On instances where it does not timeout, RONI fails to mark any instance. Interestingly, tRONI marks a small fraction of attack instances which helps correct 40% of the predictions, but still hurting the PDR. The partial success of tRONI is due to two factors: the small number of instances used in the attack and the limited Leverage for the attacker, which boosts the negative impact of attack instances through resampling. We observed that due to variance, the negative impact computed by tRONI is larger than the one perceived by the attacker for discovered instances. The adversary could adapt by increasing the confidence level of the statistic that reflects negative impact in the StingRay algorithm.

Data breach predictor: The attacks for this application correspond to two scenarios, one with limited Leverage. Indeed, the one in which the attacker has limited Leverage has a SR of 5%, while the other one has a SR of 63%. This corroborates our observation of the impact of adversarial Leverage for the exploit prediction. RONI fails due to consistent timeouts in training the Random Forest classifier. tRONI fixes 20% of the attacks while decreasing the PDR slightly. MM is a natural fit for the features based on timeseries and is able to build more balanced voting folds. The defense fixes 55% of mispredictions, at the expense of lowering the PDR to 0.91.

Our results suggest that StingRay is practical against a variety of classification tasks—even with limited degrees of Leverage. The existing defenses, where applicable, are easily bypassed by lowering the required negative impact of crafted instances. However, the reduced attack success rate on applications with limited Leverage suggests new directions for future defenses. The remainder of this section evaluates StingRay under realistic assumptions about attackers with limited knowledge and control over the victim classifier.

5.2 FAIL analysis

In this section, we evaluate the image classifier and the malware detector using the **FAIL** framework. The model allows us to utilize both StingRay as well as a state of the art evasion attack for the first task. We chose to implement the FAIL analysis on the two applications as they do not present built in Leverage limitations and they have

#	Δ	SR %	PDR	Instances	Δ	SR %	δ_D	Δ	SR %	PDR	Instances
FAIL:Unknown features											
1	39%	87/63/67	0.93/0.96/0.96	8/4/10	62%	86/7	0.054	109066	79/3/5	0.99/0.99/1.00	73/50/53
2	66%	84/71/74	0.94/0.95/0.95	8/4/9	32%	67/3	0.070	327199	77/12/13	0.99/0.99/1.00	51/50/15
FAIL:Unknown algorithm											
3	shallow	83/65/68	0.97/0.97/0.96	17/14/15	shallow	99/10	0.035	SGD	42/33/42	0.99/0.99/0.99	65/50/31
4	narrow	75/67/72	0.96/0.97/0.96	20/16/17	narrow	82/20	0.027	dSVM	38/35/48	0.99/0.99/0.99	78/50/61
FAIL:Unavailable training set											
5	35000	73/68/76	0.97/0.96/0.96	17/16/14	35000	93/18	0.032	8514	69/27/27	0.90/0.99/0.99	57/50/42
6	50000	78/70/74	0.97/0.97/0.97	18/16/15	50000	80/80	0.026	85148	50/50/50	0.99/0.99/0.99	77/50/61
FAIL:Unknown training set											
7	45000	82/69/74	0.98/0.96/0.96	16/10/15	45000	90/18	0.029	8514	53/21/24	0.93/0.99/1.00	62/50/49
8	50000	70/62/68	0.95/0.96/0.96	17/8/17	50000	96/19	0.034	43865	36/29/39	1.04/0.99/0.99	100/50/87
FAIL:Read-only features											
9	25%	80/70/72	0.97/0.97/0.97	19/16/15	18%	80/4	0.011	851	73/12/13	0.67/0.99/1.00	50/50/10
10	50%	80/71/76	0.97/0.97/0.97	18/16/13	41%	80/34	0.022	8514	49/16/17	0.90/0.99/1.00	61/50/47
11	75%	83/78/79	0.97/0.97/0.96	16/16/12	62%	80/80	0.026	85148	32/32/32	0.99/0.99/0.99	79/50/57

Table 4: StingRay on the image classifier

Table 5: JSMA on the image classifier

Table 6: StingRay on the malware classifier

Tables 4, 5, 6: FAIL analysis of the two applications. For each StingRay experiment, we report the attack success rate (SR) and PDR on the average F1 score (perceived/actual/potential), as well as statistics for the crafted instances on successful attacks (mean/median/standard deviation). For each JSMA experiment we report the attack success rate (perceived/potential), as well as the mean perturbation δ_D introduced to the evasion instances. Δ represents the variation of the **FAIL** dimension investigated.

distinct characteristics.

StingRay on the image classifier. Table 4 summarizes our results after performing all 100 attacks across 11 experiments. For each experiment, the table reports the Δ variation of the **FAIL** dimension investigated, the SR, the PDR, and the number of poison instances needed. We present three SR and PDR statistics: *perceived* (as observed by the attacker on their classifier) *actual* (as reflected on the victim when triggering the attacks perceived successful) and *potential* (the effect on the victim if all attack attempts are triggered by the attacker).

Experiments #1–2 model the case in which the attacker has limited **Feature knowledge**. This could realistically model a poisoner attacking a self-driving system who may not know if the car has narrow or wide angle cameras. We simulate this by cropping a frame of 6 and 3 pixels from the images, decreasing the available features by 61% and 34%, respectively. The attacker uses the cropped images for training and testing the classifier, as well as for crafting poison instances. On the victim classifier, the cropped part of the images is added back without altering the perturbations on poison instances. Figure 3 illustrates some example images. We observe that the perceived SR is over 84%, but the actual success rate drops significantly on the victim. However, the actual SR for #2 is similar to the white-box attacker, showing that features derived from the exterior regions of an image are less specific to an instance. This suggests that, although reducing feature knowledge decreases the effectiveness of StingRay, the specificity of some known features may still enable successful attacks.

We then model an attacker with limited **Algorithm knowledge**, possessing a similar architecture, but with

smaller network capacity. For the shallow network (#3) the attacker network has one less hidden layer; the narrow architecture (#4) has half of the original number of neurons in the fully connected hidden layers. We observe that both architectures allow the attacker to accurately approximate the deep space distance between instances. While the perceived SR is overestimated, the actual SR of these attacks is comparable to the white-box attack, showing that architecture secrecy does not significantly increase the resilience against these attacks. The open-source neural network architectures readily available for many of classification tasks would help the adversary.

Instance knowledge. In #5 we simulate a scenario where the attacker only knows 70% of the victim training set. The PDR is increased because the smaller available training set size prevents them from training a robust classifier. Experiment #6 corresponds to the white-box adversary. Here we observe that the perceived, actual and potential SRs are different. We determined that this discrepancy is caused by documented nondeterminism in the implementation framework. This affects the order in which instances are processed, causing variance on the model parameters, which in turns reflects on the effectiveness of poisoning instances. Experiments #7–8 model an attacker with 80% of the training set available and an additional subset of instances sampled from the same distribution. Surprisingly, we observe that the actual SR for #8, where the attacker has more training instances at her disposal, is lower than for #7. This is likely caused by the fact that, with larger discrepancy between the training sets of the victim and the attacker classifier, the attacker is more likely to select base instances that would not be present in the victim training set. After poison-



Figure 3: Example of base and crafted images. Images in the left panel are crafted with 10% and 20% of features unknown. In the right panel, the images are crafted with 100% and 50% leverage.

ing the victim, the effect of crafted instances would not be bootstrapped by the base instances, and the attacker fails. The results suggest that the attack is sensitive to the presence of specific pristine instances in the training set, and variance in the model parameters could mitigate the threat. However, determining which instances should be kept secret is subject for future research.

Experiments #9–11 model the case where the attacker has limited **Leverage** and is unable to modify some of the instance features. This could represent a region where watermarks are added to images to check their integrity. We simulate the attack by considering a border in the image from which the modified pixels would be discarded. This corresponds to the attacker being able to modify 25%, 50% and 75% of the image respectively. The results show an increase in the actual SR beyond the white-box attack. When discarding modified pixels, the overall perturbation is reduced. Thus, it is more likely that the poisonous samples will become more collectively inconspicuous, making the attack more effective.

The FAIL analysis results show that the perceived PDR is generally an accurate representation of the actual value, making it easy for the adversary to assess the instance inconspicuousness and indiscriminate damage caused by the attack. The attacks transfer surprisingly well from the attacker to the victim, and a significant number of failed attacks would potentially be successful if triggered on the victim. We observe that limited leverage allows the attacker to localize their strategy, crafting attack instances that are even *more successful* than the white-box attack.

Evasion attack on the image classifier. We also apply the FAIL analysis on JSMA [31], a popular targeted evasion attack for image classifiers. The transferability of the attack has previously been studied only for an adversary with limited knowledge along the **A** and **I** dimensions [33]. We attempt to reuse the same application configuration as in prior work, implementing our architecture for a handwritten digit dataset [23]. The FAIL dimensions remain identical to the analysis for StingRay. Table 5 reports the perceived and potential success rate of these attacks.

We observe in #6, that the white-box attacker could reach 80% SR. For limited **Feature knowledge** (#1–2), the perceived success is still high, but the actual SR is

very low. This suggests that the evasion attacks are very sensitive in such scenarios, highlighting a potential direction for future defenses.

For limited **Algorithmic knowledge**, we observe that the shallow architecture (#3) renders almost all attacks as successful on the attacker. However, the potential SR on the victim is higher for the narrow setup (#4). This contradicts claims in prior work [33], which state that the used architecture is not a factor for success.

On the limited **Instance knowledge** dimension, we observe that a robust attacker classifier reduces the SR to 19%. The lack of transferability hints that JSMA is highly dependent on the availability of the victim training set. We also observe a significant drop in transferability for the **L** dimension, although #11 shows that the attacker’s success is not reduced with leverage above a certain threshold.

StingRay on the malware classifier. In order to evaluate StingRay in the **FAIL** setting on the malware classifier, we trigger the 1,717 attacks on 18 dimensions. Table 6 summarizes the results. Experiment #6 corresponds to the white-box attacker. To control for additional confounding factors, in this analysis we purposely omit the negative impact-based pruning phase of the attack.

Experiments #1–2 look at the case where **Features** are unknown to the adversary. In this case, the surrogate model used to craft poison instances includes only 20% and 60% of the features respectively. Surprisingly, the attack is highly ineffective. Although the attacker perceives the attack as successful in some cases, the classifier trained on the available feature subspace is a very inaccurate approximation of the original one, resulting in an actual SR of at most 12%. These results indicate that the secrecy of features might be a viable lead towards effective defenses.

We also investigate adversaries with various degrees of knowledge about the classification Algorithm. Experiment #3 trains a linear model using the Stochastic Gradient Descent (SGD) algorithm, and in #4 (dSVM), the hyperparameters of the SVM classifier are not known by the attacker. Compared with the original Drebin SVM classifier, the default setting in #4 uses a larger regularization parameter. This suggests that regularization can help mitigate the impact of individual poison instances, but the adversary may nevertheless be successful by injecting more crafted instances in the training set.

Instance knowledge. Experiments #5–6 look at the scenario where the known **Instances** are subsets of S^* . Unsurprisingly, the attack is more effective as more instances from S^* become available. The attacker’s inability to train a robust surrogate classifier is reflected through the large perceived PDR. For experiments #7–8, victim training instances are not available to the attacker,

their classifier being trained on samples from the same underlying distribution as S^* . Under these constraints, the adversary could only approximate the effect of the attack on the targeted classifier. Additionally, the training instances might be significantly different than the base instances available to the adversary, canceling the effect of crafted instances. The results show, as in the case of the image classifier, that poison instances are highly dependent on other instances present in the training set to bootstrap their effect on target misclassification.

We further look at the impact of limited **Leverage** on the attack effectiveness. Experiments #9–11 look at various training set sizes for the case where only the features extracted from *AndroidManifest.xml* are modifiable. These features correspond to approximately 40% of the 545,333 existing features. Once again, we observe that the effectiveness of a constrained attacker is reduced. This signals that a viable defense could be to extract feature from uncorrelated sources, which would limit the leverage of such an attacker. The FAIL analysis on the malware classifier reveals that the actual drop in performance of the attacks is insignificant on all dimensions, but the attack effectiveness is generally decreased for weaker adversaries. However, feature secrecy appears to have the most significant effect on decreasing the success rate, hinting that it might be a viable defense.

6 Related work

Several studies proposed ways to model adversaries against machine learning systems. [24, 9] introduce game theoretical Stackelberg formulations for the interaction between the adversary and the data miner in the case of data manipulations. Limitations and capabilities of an adversary is discussed in [20]. Existing attacks against machine learning consider adversaries with varying degrees of knowledge, but they do not span the whole spectrum of potential adversarial knowledge [5, 31, 33]. Recent studies investigate successful transferability of the attacks conducted by limited adversaries on an auxiliary model to the actual target model [32, 25, 11]. FAIL is a unified framework for a realistic adversaries, and can be used to model the capabilities of the attackers in a systematic manner. Unlike game theoretical approaches, FAIL does not assume perfect knowledge. By capturing the wider spectrum of adversarial knowledge, FAIL model expands the existing notion of transferability as general transferability.

Existing work introduced discriminate and targeted poisoning attacks. For indiscriminate poisoning, a spammer can force a Bayesian spam filter to classify legitimate emails as spam by including a large number of dictionary words in spam emails, causing the classifier to learn that all tokens are indicative of spam [4]. An at-

tacker can degrade the performance of a Twitter-based exploit predictor by posting fraudulent tweets that mimic most of the features of informative posts [38]. An adversary can damage overall performance of a SVM classifier by injecting a small volume of specially crafted attack points [6]. For targeted poisoning, a spammer can trigger the spam filter against a specific legitimate email by crafting spam emails resembling the target email [29]. In healthcare, an adversary can subvert the predictions for a whole target class of patients by injecting fake patient data that resembles the target class [28]. StingRay is a model agnostic targeted poisoning attack, and works on a broad range of applications. Unlike existing targeted poisoning attacks, StingRay aims to bound indiscriminate damage not to degrade the overall performance. It also does not require control of the labeling function.

On neural networks, [21] proposes an targeted poisoning attack that modifies training instances which have strong influence on the target loss. In [49], the poisoning attack is a white-box indiscriminate attack adapted from existing evasion attacks. Furthermore, [26] and [18] introduce backdooring and trojaning attacks where adversaries aim to poison the classifiers to generate desired misclassification when a backdoor trigger is present in the input. Unlike these attacks, StingRay does not require white-box or query access the original model, and also it does not require modifications to test time inputs.

7 Discussion

The vulnerability of ML systems to evasion and poisoning attacks lead to an arms race, where defenses that seem promising are quickly thwarted by new attacks [16, 31, 34, 11]. Defenses proposed in the prior work make implicit assumptions about how the adversary’s capabilities should be constrained to improve the system’s resilience to attacks. The **FAIL** adversary model provides a framework for exposing and systematizing these assumptions. For example, defensive distillation [34] constrains the adversary’s knowledge along the **A** dimension, by modifying the architecture of the neural network, while RONI constrains the adversary along the **I** dimension by sanitizing the training data. The ML-based systems employed in the security industry [19, 12, 35, 13], often rely on undisclosed features to render attacks more difficult, thus constraining the **F** dimension. In Table 7 we summarize the implicit and explicit assumptions of existing poisoning and evasion attacks and defenses.

Through our systematic exploration of the **FAIL** dimensions, we provide the first experimental comparison of the importance of these dimensions for the adversary’s goals, in the context of targeted poisoning and evasion attacks. For a linear classifier, our results suggest that fea-

Work	F	A	I	L
Test Time Defenses				
Defensive Distillation[34]	•••	••	o	••
Feature Squeezing[47]	•••	••	o	oo
Adversarial Training[16]	•••	••	••	oo
Training Time Defenses				
RONI[29]	•••	oo	••	••
Micromodels[14]	••	oo	o	oo
Test Time Attacks				
Genetic Evasion[48]	••	•	oo	••
Blackbox Evasion[33]	oo	oo	•	••
Model Stealing[44]	•••	••	••	ooo
FGSM Attack[16]	•••	•••	•	oo
Carlini&Wagner Attacks[11]	ooo	••	•	••
Training Time Attacks				
Spam Filter Poisoning[29]	•••	•••	•••	••
SVM Poisoning[6]	•••	•••	•••	ooo
Healthcare Poisoning[28]	•••	ooo	••	••
Neural Network Poisoning[49]	ooo	•••	•••	oo
Neural Network Trojaning[26]	ooo	•••	••	ooo

Table 7: The analysis of FAIL dimensions attacks against machine learning. For each work, • means that the work explicitly models an adversary with no capability on the FAIL dimension, •• means an adversary with varying capability, and ••• means an adversary with full capability. Similarly, o, oo, and ooo mean the work did not consider the dimension while modeling the potential adversaries, and therefore made an implicit assumption about adversary’s capabilities in the FAIL framework. o implicitly models an adversary with no capability, oo implicitly models an adversary with partial capability and ooo implicitly models an adversary with full capability.

ture secrecy is the most promising direction for achieving attack resilience. Additionally, reducing leverage can increase the cost for the attacker. For a neural network based image recognition system, our results suggest that StingRay’s samples are transferable across all dimensions. Interestingly, limiting the leverage causes the attacker to craft instances that are more potent in triggering the attack. We also observed that training-instance secrecy provides limited resilience in this case. We demonstrated that the **FAIL** adversary model is also applicable to targeted evasion attacks. Our results suggested a lack of transferability for a state of the art classifier, while highlighting feature secrecy as the most prominent factor in reducing the attack success rate.

Future research may utilize this framework as a vehicle for reasoning about the most promising directions for defending against other attacks.

Our results also provide new insights for the broader debate about the generalization capabilities of neural networks. While neural networks have dramatically reduced test-time errors for many applications, which suggests they are capable of generalization (e.g. by learning meaningful features from the training data), recent work [51] has shown that neural networks can also mem-

orize randomly-labeled training data (which lack meaningful features). We provide a first step toward understanding the extent to which an adversary can exploit this behavior. Our results are consistent with the hypothesis that an attack such as StingRay can force selective memorization for a target instance, while preserving the generalization capabilities of the model. We leave testing this hypothesis in a rigorous manner for future work.

8 Conclusions

We introduce the **FAIL** model, a general framework for evaluating realistic attacks against machine learning systems. We also propose StingRay, a targeted poisoning attack designed to bypass existing defenses. We show that our attack is practical for 4 classification tasks, which use 3 different classifiers. By exploring the **FAIL** dimensions, we observe new transferability properties in existing targeted evasion attacks and highlight characteristics that could provide resiliency against targeted poisoning. This exploration generalizes the prior work on attack transferability and provides the first results on the transferability of poison samples.

Acknowledgments We thank Ciprian Baetu, Jonathan Katz, Daniel Marcu, Tom Goldstein, Michael Maynard, Ali Shafahi and W. Ronny Huang for their feedback. We also thank the Drebin authors for giving us access to their data set and VirusTotal for access to their service. This research was partially supported by the Department of Defense and the Maryland Procurement Office (contract H98230-14-C-0127).

Appendix

A The StingRay Attack

Algorithm 1 shows the pseudocode of StingRay’s two general-purpose procedures. `CRAFTATTACKINSTANCES` builds a set I with at least N and at most M_I attack instances. In the sample crafting loop, this procedure invokes `GETBASEINSTANCE` to select appropriate base instances for the target. Each iteration of the loop crafts one poison instance by invoking `CRAFTINSTANCE`, which modifies the set of allowable features (according to `FAIL`’s \mathbf{L} dimension) of the base instance. This procedure is specific to each application. The other application-specific elements are the distance function D and the method for injecting the poison in the training set: the crafted instances may either replace or complement the base instances, depending on the application domain. Next, we describe the steps that overcome the main challenges of targeted poisoning.

Application-specific instance modification. `CRAFTINSTANCE` crafts a poisoning instance by modifying the set of allowable features of the base instance. The procedure selects a random sample among these features, under the constraint of the target resemblance budget. It then alters these features to resemble those of the target. Each crafted sample introduces only a small perturbation that may not be sufficient to induce the target misclassification; however, because different samples modify different features, they collectively teach the classifier that the features of \mathbf{t} correspond to label y_d . We discuss the implementation details of this procedure for the four applications in Section 4.1.

Crafting individually inconspicuous samples. To ensure that the attack instances do not stand out from the rest of the training set, `GETBASEINSTANCE` randomly selects a base instance from S' , labeled with the desired target class y_d , that lies within δ_D distance from the target. By choosing base instances that are as close to the target as possible, the adversary reduces the risk that the crafted samples will become outliers in the training set. The adversary can further reduce this risk by trading target resemblance (modifying fewer features in the crafted samples) for the need to craft more poison samples (increasing N). The adversary then checks the negative impact of the crafted instance on the training set sample S' . The crafted instance \mathbf{x}_c is discarded if it changes the prediction on \mathbf{t} above the attacker set threshold δ_{NI} or added to the attack set otherwise. To validate that these techniques result in individually inconspicuous samples, we consider whether our crafted samples would be detected by three anti-poisoning defenses, discussed in detail in

Section 4.2.

Crafting collectively inconspicuous samples. After the crafting stage, `GETPDR` checks the perceived PDR on the available classifier. The attack is considered successful if both adversarial goals are achieved: changing the prediction of the available classifier and not decreasing the PDR below a desired threshold δ^{PDR} .

Guessing the labels of the crafted samples. By modifying only a few features in crafted sample, `CRAFTINSTANCE` aims to preserve the label y_d of the base instance. While the adversary is unable to dictate how the poison samples will be labeled, she may guess this label by consulting an oracle. We discuss the effectiveness of this technique in Section 4.3.

B Poisoning Defenses

Arms Race with RONI. Experimentally, we found out that for the best detection performance RONI must start by allowing a high negative impact, which means a higher threshold value, to reject the training instances that cause the most severe performance degradation. then lower the threshold for negative impact over the next iterations, as the training set becomes cleaner with each iteration.

RONI is generally effective against indiscriminate attacks, which aim to increase the false positive or false negative rates of the classifier. RONI relies on the assumption that adding poisoned instances to the training set leads to performance degradation, which tends to hold for indiscriminate attacks, as the attacker aims to induce as many mispredictions as possible.

We analyze our attack’s ability to bypass RONI while still inducing a false negative on the targeted instance.

For this, we select 13, 21, and 25 targets, respectively, for our three applications, and we craft poisoned instances for each of these targets. Figure 4 shows the dTP rate (the detection rate) of both RONI and tRONI on attack instances crafted against Drebin. These instances have a variety of negative impacts NI , computed by the attacker during sample crafting (see Algorithm 1). We group these instances into four bins. Both RONI variants fail to detect most of the attack instances with a low negative impact, and, as expected, tRONI has a higher detection rate than the baseline. In some cases, RONI is able to detect some instances with an attacker-computed impact below the detection threshold. This happens because the attacker has access to a sample of the training set, which it uses to approximate the negative impact. This sample can sometimes underestimate the negative impact of attack instances when considered in the context of the entire training set. Nevertheless, we observe

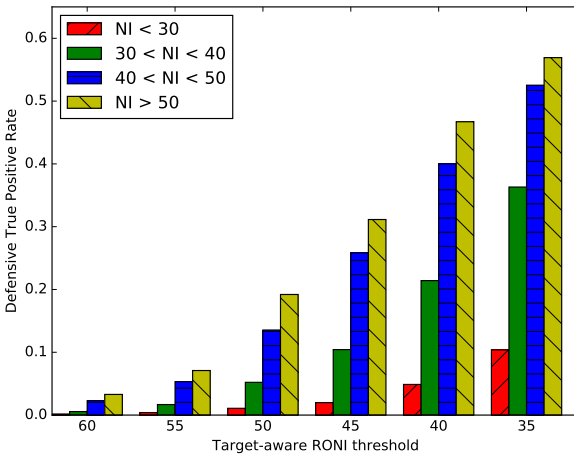
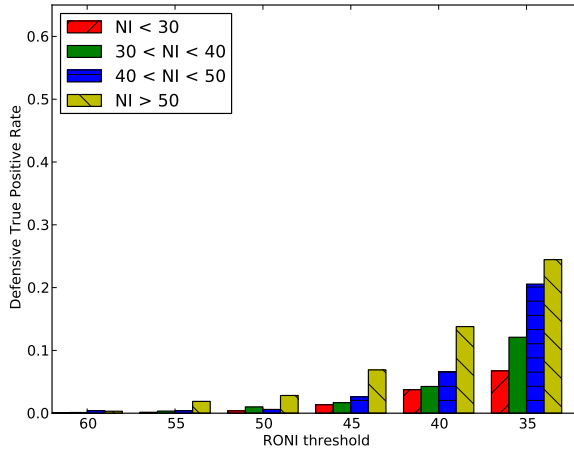


Figure 4: The percentage of crafted instances detected by RONI (top) and target-aware RONI (bottom) for decreasing thresholds of negative impact. Different instance categories correspond to different attack thresholds for the negative impact NI .

that the number of poisoned instances that RONI can detect increases in a linear fashion as we lower the impact threshold for detection.

This illustrates the arms race between RONI and our targeted poisoning attack. RONI variants (and tRONI in particular) can detect a larger portion of the poison samples as long as we lower the detection thresholds THS , which also increases the dFP rate. However, the attacker can circumvent this defense by crafting instances with a smaller negative impact. This implies that it is difficult to set the negative thresholds THS manually to achieve an adequate protection against targeted poisoning attacks.

References

- [1] Ey - the future of underwriting, 2015.
- [2] ALEXEY MALANOV 12 POSTS MALWARE EXPERT, ANTI-MALWARE TECHNOLOGIES DEVELOPMENT, K. L. The multilayered security model in kaspersky lab products, Mar 2017.
- [3] ARP, D., SPREITZENBARTH, M., HUBNER, M., GASCON, H., AND RIECK, K. Drebin: Effective and explainable detection of android malware in your pocket. In *NDSS* (2014).
- [4] BARRENO, M., NELSON, B., JOSEPH, A. D., AND TYGAR, J. D. The security of machine learning. *Machine Learning* 81 (2010), 121–148.
- [5] BIGGIO, B., CORONA, I., MAIORCA, D., NELSON, B., ŠRNĐIĆ, N., LASKOV, P., GIACINTO, G., AND ROLI, F. Evasion attacks against machine learning at test time. In *Joint European Conference on Machine Learning and Knowledge Discovery in Databases* (2013), Springer, pp. 387–402.
- [6] BIGGIO, B., NELSON, B., AND LASKOV, P. Poisoning attacks against support vector machines. *arXiv preprint arXiv:1206.6389* (2012).
- [7] BLOG, G. R. Assisting pathologists in detecting cancer with deep learning. <https://research.googleblog.com/2017/03/assisting-pathologists-in-detecting.html>, Mar 2017.
- [8] BOJARSKI, M., YERES, P., CHOROMANSKA, A., CHOROMANSKI, K., FIRNER, B., JACKEL, L., AND MULLER, U. Explaining how a deep neural network trained with end-to-end learning steers a car. *arXiv preprint arXiv:1704.07911* (2017).
- [9] BRÜCKNER, M., AND SCHEFFER, T. Stackelberg games for adversarial prediction problems. In *Proceedings of the 17th ACM SIGKDD international conference on Knowledge discovery and data mining* (2011), ACM, pp. 547–555.
- [10] CARLINI, N., AND WAGNER, D. Adversarial examples are not easily detected: Bypassing ten detection methods. In *Proceedings of the 10th ACM Workshop on Artificial Intelligence and Security* (2017), ACM, pp. 3–14.
- [11] CARLINI, N., AND WAGNER, D. Towards evaluating the robustness of neural networks. In *Security and Privacy (SP), 2017 IEEE Symposium on* (2017), IEEE, pp. 39–57.
- [12] CHAU, D. H. P., NACHENBERG, C., WILHELM, J., WRIGHT, A., AND FALOUTSOS, C. Polonium : Tera-scale graph mining for malware detection. In *SIAM International Conference on Data Mining (SDM)* (Mesa, AZ, April 2011).
- [13] COLVIN, R. Stranger danger - introducing smartscreen application reputation. <http://blogs.msdn.com/b/ie/archive/2010/10/13/stranger-danger-introducing-smartscreen-application.aspx>, Oct 2010.
- [14] CRETU, G. F., STAVROU, A., LOCASO, M. E., STOLFO, S. J., AND KEROMYTIS, A. D. Casting out demons: Sanitizing training data for anomaly sensors. In *Security and Privacy, 2008. SP 2008. IEEE Symposium on* (2008), IEEE, pp. 81–95.
- [15] FAIR ISAAC CORPORATION. FICO enterprise security score gives long-term view of cyber risk exposure, November 2016. <http://www.fico.com/en/newsroom/fico-enterprise-security-score-gives-long-term-view-of-cyber-risk-exposure> 2016.
- [16] GOODFELLOW, I. J., SHLENS, J., AND SZEGEDY, C. Explaining and harnessing adversarial examples. *arXiv preprint arXiv:1412.6572* (2014).
- [17] GRIER, C., THOMAS, K., PAXSON, V., AND ZHANG, M. @ spam: the underground on 140 characters or less. In *Proceedings of the 17th ACM conference on Computer and communications security* (2010), ACM, pp. 27–37.
- [18] GU, T., DOLAN-GAVITT, B., AND GARG, S. Badnets: Identifying vulnerabilities in the machine learning model supply chain. *arXiv preprint arXiv:1708.06733* (2017).
- [19] HEARN, M. Abuse at scale. In *RIPE 64* (Ljubljana, Slovenia, Apr 2012). <https://ripe64.ripe.net/archives/video/>.
- [20] HUANG, L., JOSEPH, A. D., NELSON, B., RUBINSTEIN, B. I., AND TYGAR, J. Adversarial machine learning. In *Proceedings of the 4th ACM workshop on Security and artificial intelligence* (2011), ACM, pp. 43–58.
- [21] KOH, P. W., AND LIANG, P. Understanding black-box predictions via influence functions. *arXiv preprint arXiv:1703.04730* (2017).
- [22] KRIZHEVSKY, A., AND HINTON, G. Learning multiple layers of features from tiny images. *Citeseer* (2009).
- [23] LECUN, Y. The mnist database of handwritten digits. <http://yann.lecun.com/exdb/mnist/> (1998).
- [24] LIU, W., AND CHAWLA, S. A game theoretical model for adversarial learning. In *Data Mining Workshops, 2009. ICDMW'09. IEEE International Conference on* (2009), IEEE, pp. 25–30.
- [25] LIU, Y., CHEN, X., LIU, C., AND SONG, D. Delving into transferable adversarial examples and black-box attacks. *arXiv preprint arXiv:1611.02770* (2016).
- [26] LIU, Y., MA, S., AAFER, Y., LEE, W.-C., ZHAI, J., WANG, W., AND ZHANG, X. Trojaning attack on neural networks. Tech. Rep. 17-002, Purdue University, 2017.
- [27] LIU, Y., SARABI, A., ZHANG, J., NAGHIZADEH, P., KARIR, M., BAILEY, M., AND LIU, M. Cloudy with a chance of breach: Forecasting cyber security incidents. In *24th USENIX Security Symposium (USENIX Security 15)* (2015), pp. 1009–1024.
- [28] MOZAFFARI-KERMANI, M., SUR-KOLAY, S., RAGHUNATHAN, A., AND JHA, N. K. Systematic poisoning attacks on and defenses for machine learning in healthcare. *IEEE journal of biomedical and health informatics* 19, 6 (2015), 1893–1905.
- [29] NELSON, B., BARRENO, M., CHI, F. J., JOSEPH, A. D., RUBINSTEIN, B. I. P., SAINI, U., SUTTON, C., TYGAR, J. D., AND XIA, K. Exploiting machine learning to subvert your spam filter. In *Proceedings of the 1st Usenix Workshop on Large-Scale Exploits and Emergent Threats* (Berkeley, CA, USA, 2008), LEET’08, USENIX Association, pp. 7:1–7:9.
- [30] PAPERNOT, N., McDANIEL, P., GOODFELLOW, I., JHA, S., CELIK, Z. B., AND SWAMI, A. Practical black-box attacks against deep learning systems using adversarial examples. *arXiv preprint arXiv:1602.02697* (2016).
- [31] PAPERNOT, N., McDANIEL, P., JHA, S., FREDRIKSON, M., CELIK, Z. B., AND SWAMI, A. The limitations of deep learning in adversarial settings. In *2016 IEEE European Symposium on Security and Privacy (EuroS&P)* (2016), IEEE, pp. 372–387.
- [32] PAPERNOT, N., McDANIEL, P. D., AND GOODFELLOW, I. J. Transferability in machine learning: from phenomena to black-box attacks using adversarial samples. *CoRR abs/1605.07277* (2016).
- [33] PAPERNOT, N., McDANIEL, P. D., GOODFELLOW, I. J., JHA, S., CELIK, Z. B., AND SWAMI, A. Practical black-box attacks against deep learning systems using adversarial examples. In *ACM Asia Conference on Computer and Communications Security* (Abu Dhabi, UAE, 2017).
- [34] PAPERNOT, N., McDANIEL, P. D., WU, X., JHA, S., AND SWAMI, A. Distillation as a defense to adversarial perturbations against deep neural networks. In *IEEE Symposium on Security and Privacy* (2016), IEEE Computer Society, pp. 582–597.

[35] RAJAB, M. A., BALLARD, L., LUTZ, N., MAVROMMATIS, P., AND PROVOS, N. CAMP: Content-agnostic malware protection. In *Network and Distributed System Security (NDSS) Symposium* (San Diego, CA, Feb 2013).

[36] REITER, E., DALE, R., AND FENG, Z. *Building natural language generation systems*, vol. 33. MIT Press, 2000.

[37] REVIEW, M. T. How to upgrade judges with machine learning. <https://www.technologyreview.com/s/603763/how-to-upgrade-judges-with-machine-learning/>, Mar 2017.

[38] SABOTTKE, C., SUCIU, O., AND DUMITRAŞ, T. Vulnerability disclosure in the age of social media: Exploiting Twitter for predicting real-world exploits. In *USENIX Security Symposium* (Washington, DC, Aug 2015).

[39] SABOTTKE, C., SUCIU, O., AND DUMITRA, T. Vulnerability disclosure in the age of social media: exploiting twitter for predicting real-world exploits. In *24th USENIX Security Symposium (USENIX Security 15)* (2015), pp. 1041–1056.

[40] SAINI, U. Machine learning in the presence of an adversary: Attacking and defending the spambayes spam filter. Tech. rep., DTIC Document, 2008.

[41] SZEGEDY, C., ZAREMBA, W., SUTSKEVER, I., BRUNA, J., ERHAN, D., GOODFELLOW, I., AND FERGUS, R. Intriguing properties of neural networks. *arXiv preprint arXiv:1312.6199* (2013).

[42] TAMERSOY, A., ROUNDY, K., AND CHAU, D. H. Guilt by association: large scale malware detection by mining file-relation graphs. In *KDD* (2014).

[43] THOMAS, K., GRIER, C., AND PAXSON, V. Adapting social spam infrastructure for political censorship. In *USENIX Workshop on Large-Scale Exploits and Emergent Threats (LEET)* (2012).

[44] TRAMÈR, F., ZHANG, F., JUELS, A., REITER, M., AND RISTENPART, T. Stealing machine learning models via prediction APIs. In *25th USENIX Security Symposium (USENIX Security 16)* (Austin, TX, Aug. 2016), USENIX Association.

[45] VERIZON. Data breach investigations reports (dbir), February 2012. <http://www.verizonenterprise.com/DBIR/>.

[46] VIRUSTOTAL. www.virustotal.com.

[47] XU, W., EVANS, D., AND QI, Y. Feature squeezing: Detecting adversarial examples in deep neural networks. *arXiv preprint arXiv:1704.01155* (2017).

[48] XU, W., QI, Y., AND EVANS, D. Automatically evading classifiers. In *Proceedings of the 2016 Network and Distributed Systems Symposium* (2016).

[49] YANG, C., WU, Q., LI, H., AND CHEN, Y. Generative poisoning attack method against neural networks. *arXiv preprint arXiv:1703.01340* (2017).

[50] YOSINSKI, J., CLUNE, J., BENGIO, Y., AND LIPSON, H. How transferable are features in deep neural networks? In *Advances in neural information processing systems* (2014), pp. 3320–3328.

[51] ZHANG, C., BENGIO, S., HARDT, M., RECHT, B., AND VINYALS, O. Understanding deep learning requires rethinking generalization. *arXiv preprint arXiv:1611.03530* (2016).

[52] ZHU, Z., AND DUMITRAS, T. Featuresmith: Automatically engineering features for malware detection by mining the security literature. In *Proceedings of the 2016 ACM SIGSAC Conference on Computer and Communications Security* (2016), ACM, pp. 767–778.